Carbohydrate Polymers 84 (2011) 1244–1251

Contents lists available at ScienceDirect

Carbohydrate Polymers

journal homepage: www.elsevier.com/locate/carbpol

Preparation and characterization of self-assembled nanoparticles of 6-*O*-cholesterol-modified chitosan for drug delivery

Mingmao Chen[a], Yan Liu[a], Wenzhi Yang[a], Xuemin Li[a], Lingrong Liu[a], Zhimin Zhou[a], Yinsong Wang[a], Ruifeng Li[a], Qiqing Zhang[a,b,*]

[a] *Institute of Biomedical Engineering, Chinese Academy of Medical Sciences & Peking Union Medical College, The Key Laboratory of Biomedical Material of Tianjin, Tianjin 300192, PR China*

[b] *Research Center of Biomedical Engineering, Xiamen University, Technology Research Center of Biomedical Engineering of Xiamen City, The Key Laboratory of Biomedical Engineering of Fujian Province, Xiamen 361005, PR China*

ARTICLE INFO

Article history:
Received 15 May 2010
Received in revised form
21 December 2010
Accepted 11 January 2011
Available online 18 January 2011

Keywords:
Chitosan
Cholesterol
Phthaloylchitosan
Self-assembled nanoparticles
All-trans retinoic acid

ABSTRACT

6-*O*-Cholesterol modified chitosan (*O*-CHCS) conjugates with succinyl linkages were synthesized through a protection-graft-deprotection method with phthaloylchitosan as an intermediate. *O*-CHCS conjugates were characterized by Fourier transform infrared spectroscopy (FTIR) and proton nuclear magnetic resonance (^{1}H NMR), and the degrees of substitution (DS) of the cholesterol moiety determined by elemental analysis were 1.7%, 4.0% or 5.9%. *O*-CHCS self-assembled nanoparticles prepared by the dialysis method displayed the classic "core–shell" structures and their sizes were in the range of 100–240 nm. All-trans retinoic acid (ATRA), as a model drug, was physically entrapped inside *O*-CHCS self-assembled nanoparticles by the dialysis method. With increasing initial levels of the drug, the drug loading content increased, but the encapsulation efficiency and the particle size decreased. The release profiles *in vitro* demonstrated that ATRA showed slow sustained released over 72 h, which indicated that *O*-CHCS self-assembled nanoparticles had the potential to be used as a carrier for hydrophobic drugs.

1. Introduction

Self-assembly of block copolymers or hydrophobically modified polymers is of growing interest with respect to biotechnology and pharmaceuticals. Amphiphilic block or graft copolymer can spontaneously form nano-sized micelle-like aggregates with an inner hydrophobic core and an outer shell of hydrophilic groups in aqueous solution (Liu, Pramoda, Yang, Chow, & He, 2004; Zhang, Ping, Zhang, & Shen, 2003). The hydrophobic core serves as a reservoir for hydrophobic drugs and the hydrophilic part serves as an interface between the bulk aqueous phase and the hydrophobic domain. Therefore, many investigations have been performed over the past decades to design and synthesize various amphiphilic polymers, especially based on natural polysaccharides (Akiyoshi et al., 1998; Kim et al., 2008; Leonard, Boisseson, Hubert, Dalencon, & Dellacherie, 2004; Na, Park, Kim, & Bae, 2000; Park et al., 2004).

Chitosan is the second most abundant, renewable natural polysaccharide after cellulose, which is composed of β-(1,4)-2-amino-2-deoxy-D-glucopyranose residues with little or no N-acetyl-D-glucosamine units (Yang et al., 2008). It is a cationic polymer with outstanding biological properties such as biocompatibility, biodegradability, non-toxicity, bioadhesiveness and antimicrobial activity. Chitosan is soluble in aqueous acidic solutions but cannot form micelles in water (Opanasopit, Ngawhirunpat, Rojanarata, Choochottiros, & Chirachanchai, 2007). In recent years, therefore, much attention has been paid to hydrophobically modified chitosan as the drug (Hu, Ren, Yuan, Du, & Zeng, 2006; Wang, Liu, Jiang, & Zhang, 2007) or gene (Lee, Kwon, Kim, Jo, & Jeong, 1998) carriers. Nevertheless, in the literature chitosan modification through amino groups is predominant. Chemical modifications of this type may change the fundamental skeleton of chitosan especially with high degree of substitution, and the modified chitosan loses the original physicochemical and biochemical activities (Sugimoto, Morimoto, Sashiwa, Saimoto, & Shigemasa, 1998). On the other hand, modification of chitosan through hydroxyl groups may have an advantage because there may be less influence on the fundamental skeleton (Gorochovceva & Makuška, 2004) and it preserves free amino groups of chitosan which play an important role in biological activity and cationic polymer properties (Liu, Li, Fang, & Chen, 2005).

* Corresponding author at: Institute of Biomedical Engineering, Chinese Academy of Medical Sciences & Peking Union Medical College, The Key Laboratory of Biomedical Material of Tianjin, Tianjin 300192, PR China.
Tel.: +86 22 87890868; fax: +86 22 87890868.
E-mail address: zhangqiq@xmu.edu.cn (Q. Zhang).

0144-8617/$ – see front matter © 2011 Elsevier Ltd. All rights reserved.
doi:10.1016/j.carbpol.2011.01.012

Cholesterol is an indispensable structural building block in cells and plays an important role in many body functions. It is often used to hydrophobically modify biomaterials because of its rigidity and highly hydrophobic sterol skeleton (Akiyoshi, Deguchi, Moriguchi, Yamaguchi, & Sunamoto, 1993; Akiyoshi et al., 1998; Yuan, Li, & Yuan, 2006). Previously, our group has reported that self-assembled nanoparticles of *N*-cholesterol-modified chitosan (*N*-CHCS) were irregularly spherical in shape with a bumpy surface due to the chain rigidity of chitosan arising from various hydrogen bonds such as O-3···O-5 (intramolecular) and N-2···O-6 (intermolecular) (Wang et al., 2007a; Wang, Liu, Weng, & Zhang, 2007). In order to weaken these hydrogen bonds, retain the fundamental skeleton and free amino groups of chitosan, in this study, 6-*O*-cholesterol modified chitosan (*O*-CHCS) conjugates with succinyl linkages were synthesized through a protection-graft-deprotection method with phthaloylchitosan (PHCS) as an intermediate. Here PHCS, phthaloyl group of which could be easily deprotected to generate free amino groups, was prepared as a key intermediate for the further grafting reaction (Kurita, Shimada, Nishiyama, Shimojoh, & Nishimura, 1998; Makuška & Gorochovceva, 2006; Yoksan, Akashi, Biramontri, & Chirachanchai, 2001). Furthermore, *O*-CHCS self-assembled nanoparticles were prepared by the dialysis method and all-trans retinoic acid (ATRA) was chosen as a model drug to estimate the potential of *O*-CHCS nanoparticles as a novel carrier for hydrophobic drugs. As an active metabolite of retinol, ATRA has been shown to exert anti-tumor activities against a number of cancer cells and tissues. However, ATRA has poor aqueous solubility, short half-lives in blood and serious side effects such as retinoid resistance, hypertriglyceridemia and headache extremely (Jeong et al., 2004; Jeong et al., 2006). Therefore, ATRA was loaded into *O*-CHCS self-assembled nanoparticles in order to sustain its release, enhance its therapeutic index and reduce its toxicity.

2. Materials and methods

2.1. Materials

Biomedical grade chitosan (M_w = 100 kDa, degree of deacetylation 87%) was supplied by Jinqiao Biochemical Co., Ltd. (Zhejiang, China). Phthalic anhydride, N-hydroxyl succinimide (NHS) and pyrene were purchased from Sigma–Aldrich (St. Louis, MO). 1-(3-Dimethylaminopropyl)-3-ethylcarbodiimide hydrochloride (EDC·HCl) was supplied by Shanghai Medpep Co., Ltd. (Shanghai, China). All-trans retinoic acid (ATRA) was purchased from Kunming Mingren Chemical Plant (Kunming, China). All other chemical reagents were analytical grade and obtained from commercial sources.

2.2. Phthaloylation of chitosan

Synthesis was carried out according to a previously reported procedure (Kurita, Ikeda, Yoshida, Shimojoh, & Harata, 2002; Rout, Pulapura, & Gross, 1993). Briefly, chitosan (1.0 g, 6.0 mmol) was mixed with excess phthalic anhydride (2.66 g, 18.0 mmol) in 20 mL of N,N-dimethyl formamide (DMF) containing 5% (v/v) water and the mixture was heated in nitrogen at 120 °C with stirring. After reaction for 7 h, the mixture was cooled to room temperature and poured into iced water. The precipitate was filtered and washed with methanol. The degree of substitution (DS) of phthaloyl group was 86% determined by elemental analysis (Heraeus CHN-O-Rapid, Germany).

2.3. Synthesis of cholesterol succinate

Cholesterol succinate (CHS) was prepared as previously described (Wang et al., 2007a). Cholesterol (2.0 g, 5.2 mmol) was added to succinic anhydride (1.56 g, 15.6 mmol) in 12 mL of pyridine. The mixture was stirred for 72 h at 45 °C and then precipitated in the iced dilute hydrochloric acid solution. CHS was obtained by recrystallization in ethyl acetate and ethanol.

2.4. Synthesis of O-CHCS

CHS (0.5 g, 1.0 mmol) in 50 mL of DMF was activated by addition EDC (0.21 g, 1.1 mmol) and NHS (0.12 g, 1.0 mmol) for 2 h. PHCS (0.92 g, 3.3 mmol) was added to the above mixture and the reaction was continued for 72 h at 45 °C. Following this, the mixture was precipitated in ethanol, then filtered and washed with ethanol, tetrahydrofuran (THF) and diethyl ether, respectively to obtain phthaloyl protected graft copolymer (PHCS–CHS).

To a solution of PHCS–CHS (0.5 g, 0.65 mmol) in 5 mL of DMF was added 30 mL of hydrazine hydrate, and the mixtrue was stirred in nitrogen at 90 °C. After 7 h of reaction, the solution was cooled to room temperature and precipitated. Then, the precipitate was collected, washed thoroughly with ethanol and distilled water, and dried in vacuum to obtain *O*-CHCS. The chemical structure of *O*-CHCS was determined by Fourier transform infrared spectroscopy (FTIR, Nicolet Nexus 470-ESP, USA) and proton nuclear magnetic resonance (^{1}H NMR, Varian Inova500, USA) using D_2O/CD_3COOD or DMSO as the solvents. DS of the cholesterol moiety was determined by elemental analysis (Heraeus CHN-O-Rapid, Germany).

2.5. Preparation of O-CHCS self-assembled nanoparticles

O-CHCS self-assembled nanoparticles were prepared by a dialysis method. Briefly, *O*-CHCS was dissolved in 0.1 M acetic acid, and then the solution was dialyzed against physiological saline for 24 h. The dialyzed liquids were exchanged every hour for the first 3 h and each 3 h for the next 21 h (Yuan et al., 2006). The morphology of *O*-CHCS self-assembled nanoparticles was observed using transmission electron microscope (TEM, JEM-100CXII, Japan). The particle size, size distribution and zeta potential of nanoparticles were measured by dynamic laser light scattering (DLLS, Malvern Nano-ZS, UK).

2.6. Measurement of fluorescence spectroscopy

The self-aggregation property of *O*-CHCS and its critical micelle concentration (CMC) were determined using fluorescence spectroscopy with pyrene as a fluorescent probe (Amiji, 1995). The pyrene solutions (3.0×10^{-4} mol/L) in methanol were added into a series of test tubes and evaporated under a stream of nitrogen gas to remove the solvents. Then, various concentrations of *O*-CHCS suspension solutions were added to each test tube, and the final concentration of pyrene was 6.0×10^{-7} mol/L. The mixture solutions were sonicated for 30 min in an ultrasonic bath (KQ-100DY, China). Pyrene emission spectra were recorded using fluorescence spectrophotometer (Shimadzu F-4500, Japan). The probe was excited at 333 nm, and the emission spectra were obtained in the range of 350–450 nm at an integration time of 1.0 s. The slit width for excitation and emission were 10 and 2.5 nm, respectively.

2.7. Preparation of ATRA-loaded O-CHCS self-assembled nanoparticles

ATRA-loaded *O*-CHCS self-assembled nanoparticles were prepared according to the method previously reported (Kim et al., 2006). ATRA dissolved in 1 mL of DMSO was dropped into 10 mL of *O*-CHCS nanoparticle suspension with ultrasonication (Automatic Ultrasonic Processor UH-500A, China) at an output power of 50 W for 2 min, in which the pulse was cycled on and off at 2 s intervals under ice temperature condition. Following this, the mixture solution was dialyzed against deionized water and the medium was replaced several times over a 9 h period. The physicochemical char-

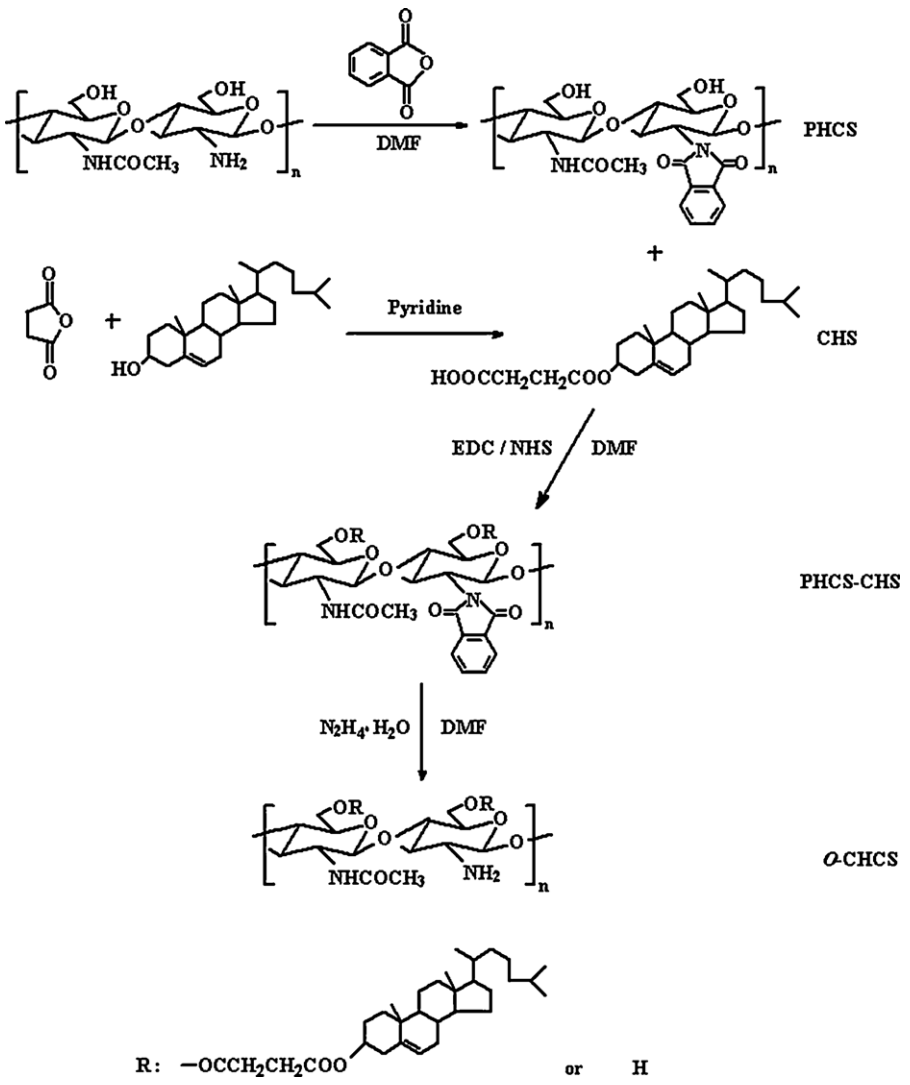

Fig. 1. Synthesis route of *O*-CHCS.

acteristics of ATRA-loaded *O*-CHCS self-assembled nanoparticles were also studied by the above methods in Section 2.5.

To determinate the drug loading content and the encapsulation efficiency, the volume of the dialyzed solution was adjusted to 20 mL by adding distilled water and then 100 μL of the solution was diluted with 10 mL of 2% acetic acid solution. Empty *O*-CHCS self-assembled nanoparticle solution was used as the reference. The ATRA loading content and encapsulation efficiency of *O*-CHCS nanoparticles were measured using UV spectrophotometer (UV-384 plus, Molecular Devices Corporation, USA) at 360 nm and calculated by using Eqs. (1) and (2), respectively:

$$\text{drug loading content} = \frac{\text{the amount of ATRA in the nanoparticles}}{\text{total amount of nanoparticle weight}} \times 100 \quad (1)$$

$$\text{encapsulation efficiency} = \frac{\text{the amount of ATRA in the nanoparticles}}{\text{total amount of ATRA}} \times 100 \quad (2)$$

2.8. Differential scanning calorimetry (DSC) analysis

DSC analysis was performed using Modulate DSC (MDSC 2910, USA). The measurements were carried out in the temperature range of 50–200 °C under nitrogen at a scanning rate of 10 °C/min.

2.9. In vitro drug release study

ATRA release behavior from *O*-CHCS self-assembled nanoparticles was studied by the dialysis method (Jeong et al., 2004; Jeong et al., 2006). Briefly, 2 mL of ATRA-loaded nanoparticle solution was introduced into a dialysis tube (Millipore dialysis tube, molecular weight cut-off 12–14 kDa) and the dialysis tube was immersed in 30 mL of phosphate buffered saline (PBS, pH 7.4). Release experiments were performed at 37 °C in an air-bath shaker at 100 rpm. At predefined time intervals, the release media were collected and the fresh release media were then added. The release amount of ATRA was measured at 360 nm with UV spectrophotometer (UV-384 plus, Molecular Devices Corporation, USA).

3. Results and discussion

3.1. Synthesis and characterization of O-CHCS

The amino groups in chitosan are responsible for many of its advanced functions, including biological activity and cationic polymer properties (Liu et al., 2005b). On the other hand, chitosan

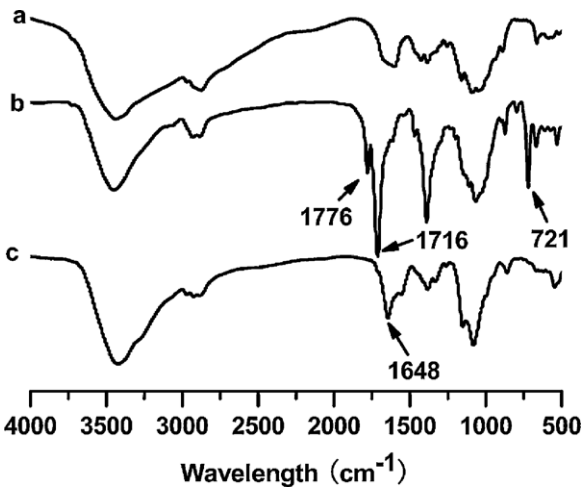

Fig. 2. IR spectra of chitosan (a), PHCS–CHS (b) and *O*-CHCS-4.0 (c).

derivatives with free amino groups can be used as useful intermediates for further chemical modifications or cross-linking. To retain free amino groups of chitosan, we focused on the regioselective grafting of cholesterol onto chitosan through a protection-graft-deprotection route. As shown in Fig. 1, amino groups of chitosan were firstly protected by phthaloyl groups, and then cholesterol modified moieties were grafted onto chitosan at the C-6 position of glucosamine units, and finally phthaloyl groups were deprotected in hydrazine hydrate to obtain *O*-CHCS. In this study, phthaloyl groups were used for protecting the amino groups of chitosan for the following two reasons (Liu et al., 2005b; Rout et al., 1993). Firstly, introduction of phthaloyl groups could reduce inter- and intra-hydrogen bonds of chitosan, which improved its solubility in organic solvents such as pyridine, DMSO and DMF. Secondly, phthaloyl groups of phthaloylchitosan could be easily deprotected to regenerate the free amino groups after cholesterol was grafted onto PHCS.

Fig. 2 showed FTIR spectra of chitosan, PHCS–CHS and *O*-CHCS. The absorption band at 1648 cm^{-1} was attributed to the carbonyl of acetyl group of chitosan (Osman & Arof, 2003). Compared with chitosan, this peak of *O*-CHCS increased, which implied that cholesterol succinate had been successfully grafted onto the chitosan backbone. The most characteristic phthalimido peaks of PHCS–CHS appeared at 1776 cm^{-1}, 1716 cm^{-1} (carbonyl anhydride) and 721 cm^{-1} (phenyl ring), but disappeared in the spectrum of *O*-CHCS, which suggested the successful removal of the phthaloyl groups from PHCS–CHS.

In this study, ^{1}H NMR was investigated to further confirm the chemical structure of the graft copolymers. Fig. 3 showed the ^{1}H NMR spectra of chitosan, PHCS, PHCS–CHS and *O*-CHCS. The characteristic peaks of chitosan (Fig. 3a) appeared at 2.7–5.0 ppm, and the characteristic aromatic phthalimido peaks of PHCS (Fig. 3b) appeared at 7.6–8.0 ppm. Compared with chitosan and PHCS, new peaks in PHCS–CHS spectrum (Fig. 3c) appeared in the range of 0.6–1.0 ppm due to the hydrogen protons of cholesterol moiety, which suggested that cholesterol modified groups were successfully grafted onto the chitosan backbone. As shown in ^{1}H NMR spectrum of *O*-CHCS (Fig. 3d), the disappearance of peaks of aromatic rings compared to PHCS–CHS indicated that the phthaloyl groups were successfully removed through deprotection reaction; the obvious increase of peaks at around 1.7 ppm and the relatively small peaks appeared in the range of 2.4–2.8 ppm compared to chitosan were assigned to the cholesterol modified groups, which indicated that the deprotection reaction would not affect the chemical conjugation of cholesterol moieties and chitosan.

Due to the self-aggregation behavior of *O*-CHCS in aqueous media, ^{1}H NMR investigation could not be used to determine DS of the cholesterol moiety (Kim, Lee, & Kang, 2000). Thus, DS of the cholesterol moiety were measured by elemental analysis and the results were listed in Table 1. It clearly showed that DS value increased from 1.7 to 5.9 per 100 anhydroglucosamine units of chitosan with the mole equivalent of CHS/PHCS increasing from 20/100 to 40/100.

3.2. Self-aggregation behavior of O-CHCS

The aggregation behavior of *O*-CHCS in aqueous media was monitored by the fluorescence probe technique in the presence of pyrene as a fluorescent probe. Pyrene is poorly soluble and a self-quenching agent in a polar environment but strongly emits radiation when micelles or other hydrophobic microdomains are formed in an aqueous solution, as it preferably lies close to (or inside) the microdomains (Amiji, 1995; Gao et al., 2008). There are five peaks in the emission spectra of pyrene, and the emission intensity ratio of the first peak (372 nm) and the third peak (383 nm) I_{372}/I_{383} is sensitive to the polarity of the microenvironment. Thus the change in peak I_{372}/I_{383} ratio of pyrene monomer fluorescence could be used to examine the aggregation behavior of surfactants or polymers in aqueous solution (Sui, Song, Chen, & Xu, 2005). The critical micelle concentration (CMC), which is the threshold concentration of self-aggregation formation by intra- and/or intermolecular association, can be determined from the change in the intensity ratio (I_{372}/I_{383}) of the pyrene in the presence of polymeric amphiphiles.

Fig. 4 showed the changes of the I_{372}/I_{383} values as a function of *O*-CHCS concentrations. The I_{372}/I_{383} values were nearly unchanged at low concentration of *O*-CHCS, but the intensity ratios dropped dramatically beyond a specific concentration of *O*-CHCS. Therefore, CMC could be determined by the interception of two straight lines. As shown in Table 1, the CMC values of *O*-CHCS in aqueous solution were in the range of 0.0072–0.0175 mg/mL, which were much lower than those of low molecular weight surfactants (Kim et al., 2005; Rahman & Brown, 1983). It indicated that *O*-CHCS showed self-aggregation behavior in aqueous solution. Furthermore, the CMC values decreased with DS of cholesterol moiety increasing, resulting from the hydrophobicity increase of inner core with the DS increase. These results were consistent with other earlier reports (Gao et al., 2008; Kwon, Park, Chung, Kwon, & Jeong, 2003; Li et al., 2006).

3.3. Preparation of O-CHCS self-assembled nanoparticles and drug loading

In this study, *O*-CHCS self-assembled nanoparticles were prepared by dialysis. As shown in Fig. 5, the morphology of *O*-CHCS nanoparticles observed by TEM was almost spherical shape with a classic core–shell structure, which proved that *O*-CHCS could form self-aggregates in the aqueous media. Table 1 summarized the characteristics of *O*-CHCS self-assembled nanoparticles. The mean diameters of *O*-CHCS self-assembled nanoparticles determined by DLLS were in the range of 100–240 nm depending on DS of the cholesterol moiety. The size of nanoparticles decreased as DS of the cholesterol moiety increased, which indicated the formation of more compact hydrophobic cores (Akiyoshi, Deguchi, Tajima, Nishikawa, & Sunamoto, 1997). The zeta potentials of *O*-CHCS self-assembled nanoparticles with different DS of the cholesterol moiety were similar and obvious positive in distilled water, which suggested that this nanoparticle system would be stable (Chen et al., 2009) in aqueous media due to the positive charged amino groups of chitosan shells.

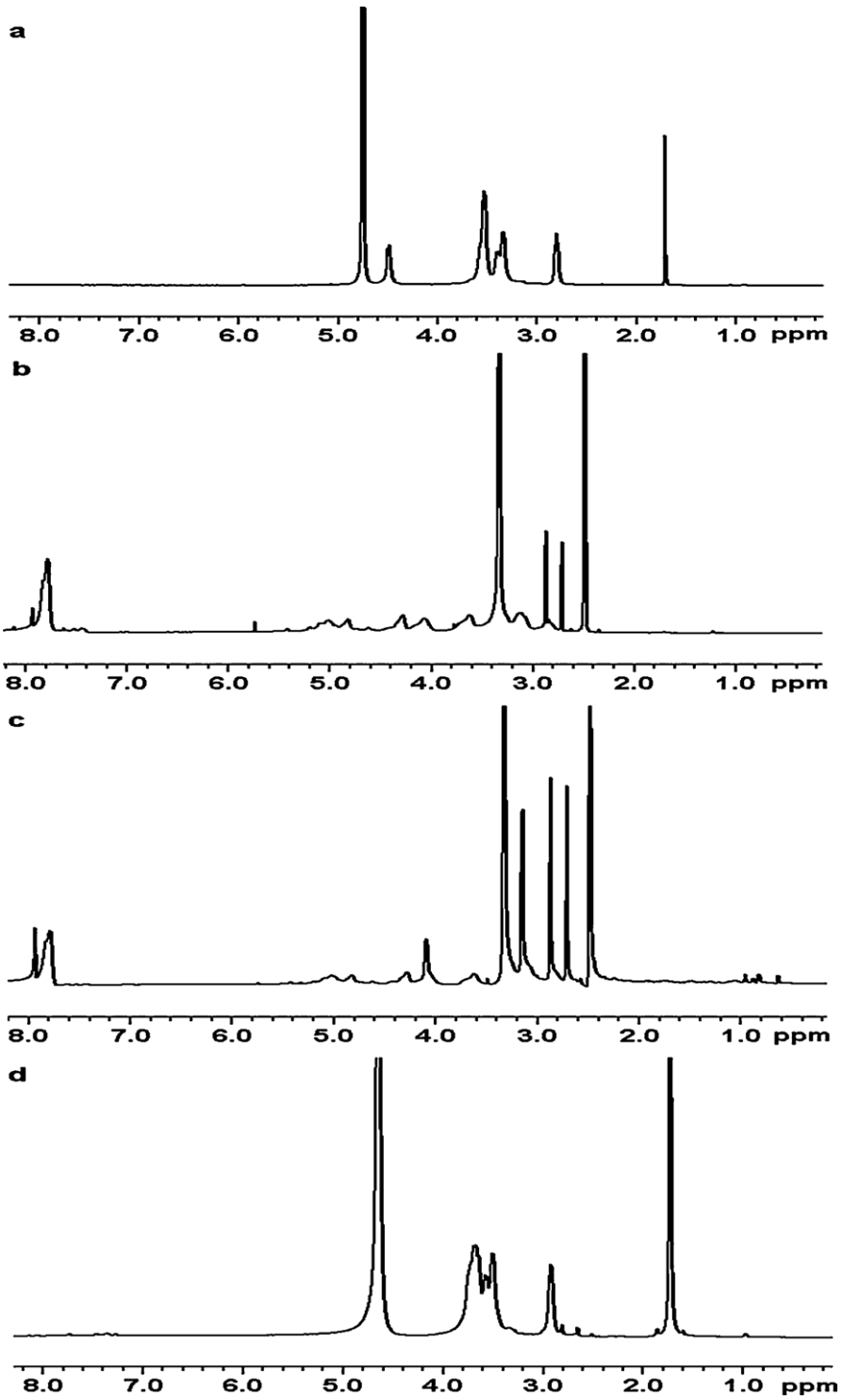

Fig. 3. ^{1}H NMR spectra of chitosan in D_2O/CD_3COOD (a), PHCS (b), PHCS–CHS in DMSO (c) and *O*-CHCS-4.0 in D_2O/CD_3COOD (d).

Table 1
Properties of *O*-CHCS.

Sample	Mole equivalent: CHS/PHCS	DS[a]	CMC ($\times 10^{-2}$ mg/mL)[b]	Mean diameter (nm)[c]	Polydispersity Index[c]	Zeta potential (mV)[c]
O-CHCS-1.7	20/100	1.7	1.75	238.5 ± 7.88	0.391 ± 0.025	+24.5 ± 0.289
O-CHCS-4.0	30/100	4.0	0.86	172.7 ± 1.266	0.193 ± 0.006	+25.6 ± 0.850
O-CHCS-5.9	40/100	5.9	0.72	101.9 ± 4.652	0.326 ± 0.064	+25.9 ± 0.495

[a] DS of CHS per 100 anhydroglucosamine units of chitosan measured by elemental analysis.
[b] The critical micelle concentration (CMC) were determined by fluorescence spectroscopy.
[c] The size, size distribution and zeta potential (mean value ± SD) determined by DLLS with three times.

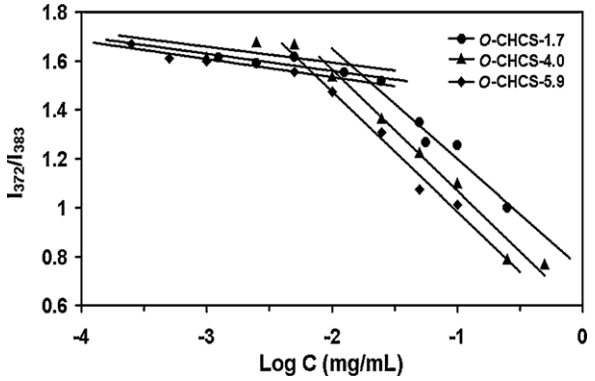

Fig. 4. The relationship of I_{372}/I_{383} from fluorescence probe spectra with log C of *O*-CHCS.

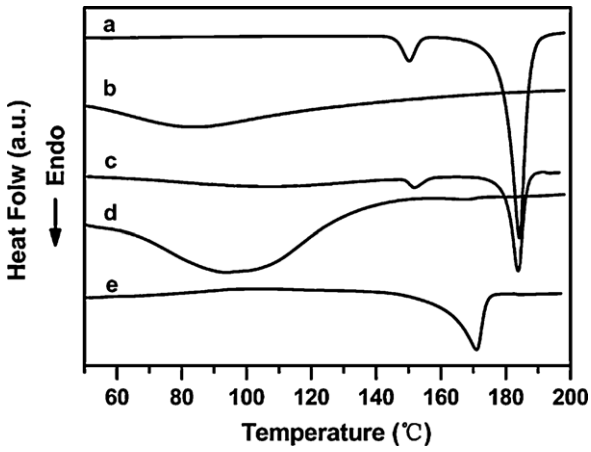

Fig. 7. DSC thermograms of ATRA (a), *O*-CHCS-4.0 nanoparticles (b), physical mixture of ATRA and *O*-CHCS-4.0 nanoparticles (1:10, w/w) (c), ATRA-loaded *O*-CHCS-4.0 nanoparticles with drug loading content of 8.0% (d) and ATRA-loaded *O*-CHCS-4.0 nanoparticles with drug loading content of 24.3% (e).

According to the previous reports (Jeong et al., 2006; Liu, Desai, Chen, & Park, 2005; Zhang et al., 2003), polymeric micelle had a hydrophilic shell and a hydrophobic core. Hence, *O*-CHCS self-assembled nanoparticle was composed of a hydrophobic core of cholesterol moieties and a hydrophilic outer-shell of chitosan backbones, as shown in Fig. 6. It was reported that the core of *N*-CHCS self-assembled nanoparticles was N-2 position with the hydrophobic cholesterol moieties (Wang et al., 2007a; Yuan et al., 2006). However, on the basis of the above experimental results, C-6 position with the hydrophobic cholesterol moieties was in the core of *O*-CHCS self-assembled nanoparticles and the hydrophilic amino groups were on the outer-shell. In addition, according to the previously reported by Kumar et al. (2004), *O*-CHCS was more flexible than chitosan by preventing the formation of hydrogen bonds (N-2 · · · O-6). Therefore, *O*-CHCS self-assembled nanoparticles had a more regular spherical shape, a more apparent core–shell structure, a smaller size and a more compact hydrophobic core, compared to *N*-CHCS self-assembled nanoparticles.

Table 2 showed the characteristics of ATRA-loaded *O*-CHCS self-assembled nanoparticles. The ATRA loading content increased from 8.0% to 28.3% with the weight ratio of ATRA to *O*-CHCS nanoparticles at the drug loading stage increasing from 1/10 to 1/2, but the encapsulation efficiency decreased at the same time. It was also clearly shown that the size of ATRA-loaded nanoparticles decreased from 222 to 190.9 nm with ATRA loading content increasing, which was not consistent with other drug nanocarriers (Jeong et al., 2003; Lee, Kim, Kwon, & Jeong, 2000; Wang et al., 2007a; Yang et al., 2008). According to the explanation reported by Tang et al. (2007), the reason explained for this difference was that the cyclohexenyl groups of ATRA inserted into the hydrophobic core of *O*-CHCS nanoparticles, and therefore the hydrophobic interaction among the hydrophobic core of the nanoparticles enhanced accordingly. Considering the size and the drug loading property, 2/5 (drug/carrier) was the optimal weight ratio to prepare ATRA-loaded *O*-CHCS self-aggregated nanoparticles.

3.4. Differential scanning calorimetry (DSC) analysis

Fig. 7 showed DSC thermograms of ATRA, *O*-CHCS nanoparticles, physical mixture of ATRA and *O*-CHCS nanoparticles (1/10, w/w), ATRA-loaded *O*-CHCS nanoparticle systems with the drug loading contents of 8.0% and 24.3%, respectively. The DSC curve of ATRA

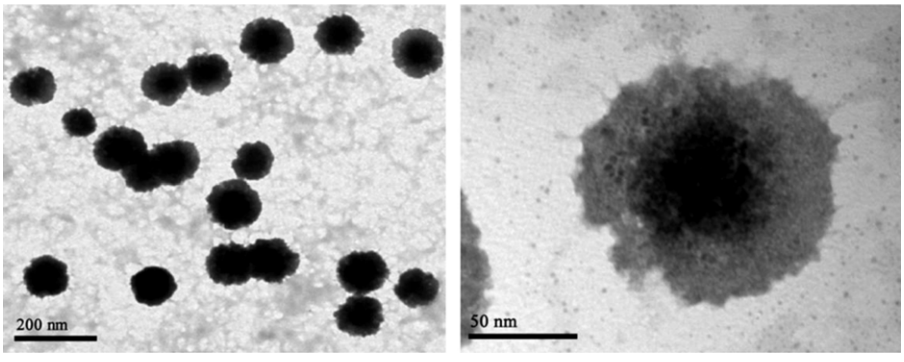

Fig. 5. TEM images of *O*-CHCS-4.0 self-assembled nanoparticles.

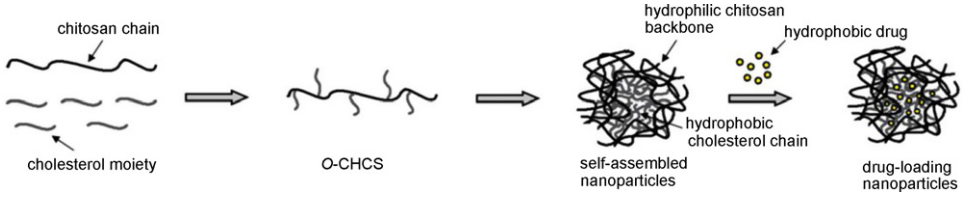

Fig. 6. Hypothetical mechanism of hydrophobic drug entrapment into self-assembled nanoparticles prepared using a dialysis method.

Table 2
Characteristics of ATRA-loaded *O*-CHCS self-assembled nanoparticles.

Drug/carrier[a]	Mean diameter (nm)[b]	Polydispersity Index[b]	Loading content (%)[c]	Encapsulation efficiency (%)[c]
1/10	222.2 ± 1.896	0.132 ± 0.025	8.0 ± 0.20	88.7 ± 1.32
1/5	204.1 ± 2.875	0.207 ± 0.020	11.8 ± 2.10	82.3 ± 1.41
2/5	190.9 ± 1.474	0.181 ± 0.004	24.3 ± 1.47	77.9 ± 1.29
1/2	192.0 ± 2.259	0.191 ± 0.008	28.3 ± 0.76	74.0 ± 0.55

[a] ATRA/*O*-CHCS-4.0 self-assembled nanoparticles (mg/mL).
[b] The size and distribution of ATRA-loaded *O*-CHCS-4.0 self-assembled nanoparticles (mean value ± SD) determined by DLLS with three times.
[c] ATRA loading content and the encapsulation efficiency (mean value ± SD) determined by UV spectrophotometer with three times.

(Fig. 7a) showed an endothermic melting peak at 184 °C, while blank *O*-CHCS nanoparticles (Fig. 7b) had only a broad peak at about 83 °C. Compared with ATRA, the DSC curve of the physical mixture of ATRA and *O*-CHCS nanoparticles (Fig. 7c) also had ATRA melting peak at 183 °C. However, the thermograms of the ATRA-loaded nanoparticles with lower and higher ATRA loading contents were clearly identical. The endothermic peak was not observed in DSC curve at lower ATRA loading content (Fig. 7d), which indicated that ATRA was wholly encapsulated into the hydrophobic cores of *O*-CHCS nanoparticles and existed as a molecular dispersion inside the nanoparticles. On the other hand, the endothermic peak appeared at 170 °C in DSC curve at higher ATRA loading content (Fig. 7e). It might be due to the crystallization of part of ATRA in nanoparticles during the drug loading process, which resulted from the appearance of phase separation at higher drug loading (Jeong et al., 1998; Jeong et al., 2002). Moreover, compared with ATRA, the melting peak of ATRA-loaded nanoparticle with higher ATRA loading content (Fig. 7e) shifted to a lower temperature (170 °C), implying that the interaction between *O*-CHCS nanoparticles and ATRA molecules could have occurred (Lira, Nanclares, Neto, & Marchetti, 2007; Sarmento, Ferreira, Veiga, & Ribeiro, 2006).

3.5. In vitro drug release studies

Fig. 8 showed ATRA release curves of ATRA loaded *O*-CHCS nanoparticles with different drug loading contents. All release profiles showed that the release behavior of ATRA from *O*-CHCS nanoparticles was initially rapid and then very slow after 20 h, which was consistent with the phenomena reported by other authors (Chen et al., 2009; Yang et al., 2008; Zhang et al., 2009). Ordinarily, drug release from particle carriers followed more than one type of mechanisms. The initial burst of ATRA from nanoparticles suggested some part of the drug was absorbed onto the surface of nanoparticles since adsorbed drug instantaneously dissolved when it contacted the release medium. The following slow and uniform release of ATRA could be due to the diffusion of the entrapped drug in nanoparticles. Another explanation for the slow drug release was the electrostatic interaction between the amino groups of chitosan and the carboxyl groups of ATRA, according to a previous report (Jeong et al., 2006).

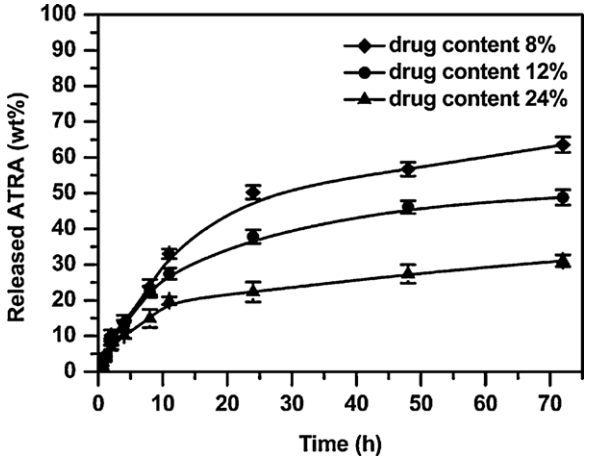

Fig. 8. ATRA release profiles from *O*-CHCS-4.0 nanoparticles in PBS (pH 7.4) at 37 °C.

In Fig. 8, it was also observed that the lower drug release rate corresponding to the higher drug loading content, which was consistent with that previously reported (Gref et al., 1994; Jeong et al., 2003). At the higher drug loading content, the hydrophobic drug crystallized inside the nanoparticles and phase separation occurred, which reduced the drug release rate. This explanation was supported by the DSC results as discussed above in Section 3.4. It was clearly showed that ATRA was sustained released from *O*-CHCS nanoparticles for more than 72 h, which suggested *O*-CHCS self-assembled nanoparticles had a potential as a sustained release carrier for ATRA.

4. Conclusions

6-*O*-Cholesterol modified chitosan derivatives (*O*-CHCS) were synthesized with phthaloylchitosan (PHCS) as an intermediate and their self-assembled nanoparticles were prepared by the dialysis method. *O*-CHCS self-assembled nanoparticles had the regular spherical shape and the classic core–shell structure. The drug loading and release experiments showed that *O*-CHCS self-assembled nanoparticles had the potential to be used as a carrier for ATRA. Therefore, this novel nanoparticle system may be useful in the delivery of hydrophobic drugs, and the further investigations are in progress.

Acknowledgements

This research was supported by the National Key Scientific Projects of China (2006CB933300) and Natural Science Foundation of China (90923042).

References

Akiyoshi, K., Deguchi, S., Moriguchi, N., Yamaguchi, S., & Sunamoto, J. (1993). Self-aggregates of hydrophobized polysaccharides in water. Formation and characteristics of nanoparticles. *Macromolecules*, *26*, 3062–3068.
Akiyoshi, K., Deguchi, S., Tajima, H., Nishikawa, T., & Sunamoto, J. (1997). Microscopic structure and thermoresponsiveness of a hydrogel nanoparticle by self-assembly of a hydrophobized polysaccharide. *Macromolecules*, *30*, 857–861.
Akiyoshi, K., Kobayashi, S., Shichibe, S., Mix, D., Baudys, M., Kim, S. W., et al. (1998). Self-assembled hydrogel nanoparticle of cholesterol-bearing pullulan as a carrier of protein drugs: Complexation and stabilization of insulin. *Journal of Controlled Release*, *54*(3), 313–320.
Amiji, M. M. (1995). Pyrene fluorescence study of chitosan self-association in aqueous solution. *Carbohydrate Polymers*, *26*, 211–213.
Chen, H. L., Yang, W. Z., Chen, H., Liu, L. R., Gao, F. P., Yang, X. D., et al. (2009). Surface modification of mitoxantrone-loaded PLGA nanospheres with chitosan. *Colloids and Surface B: Biointerfaces*, *73*, 212–218.
Gao, F. P., Zhang, H. Z., Liu, L. R., Wang, Y. S., Jiang, Q., Yang, X. D., et al. (2008). Preparation and physicochemical characteristics of self-assembled nanoparticles of deoxycholic acid modified-carboxymethyl curdlan conjugates. *Carbohydrate Polymers*, *71*, 606–613.
Gorochovceva, N., & Makuška, R. (2004). Synthesis and study of water-soluble chitosan-O-poly(ethylene glycol) graft copolymers. *European Polymer Journal*, *40*, 685–691.

Gref, R., Minamitake, Y., Peracchia, M. T., Trubetskoy, V., Torchilin, V., & Langer, R. (1994). Biodegradable long-circulating polymeric nanospheres. *Science*, *263*, 1600–1603.

Hu, F. Q., Ren, G. F., Yuan, H., Du, Y. Z., & Zeng, S. (2006). Shell cross-linked stearic acid grafted chitosan oligosaccharide self-aggregated micelles for controlled release of paclitaxel. *Colloids and Surface B: Biointerfaces*, *50*, 97–103.

Jeong, Y. I., Cheon, J. B., Kim, S. H., Nah, J. W., Lee, Y. M., Sung, Y. K., et al. (1998). Clonazepam release from core–shell type nanoparticles in vitro. *Journal of Controlled Release*, *51*, 169–178.

Jeong, Y. I., Kang, M. K., Sun, H. S., Kang, S. S., Kim, H. W., Moon, K. S., et al. (2004). All-trans-retinoic acid release from core–shell type nanoparticles of poly(epsilon-caprolactone)/poly(ethylene glycol) diblock copolymer. *International Journal of Pharmaceutics*, *273*(1–2), 95–107.

Jeong, Y. I., Kim, S. H., Jung, T. Y., Kim, I. Y., Kang, S. S., Jin, Y. H., et al. (2006). Polyion complex micelles composed of all-trans retinoic acid and poly (ethylene glycol)-grafted-chitosan. *Journal of Pharmaceutical Sciences*, *95*(11), 2348–2360.

Jeong, Y. I., Shim, Y. H., Song, K. C., Park, Y. G., Ryu, H. W., & Nah, J. W. (2002). Testosterone-encapsulated surfactant-free nanoparticles of poly(DL-lactide-co-glycolide): Preparation and release behavior. *Bulletin of the Korean Chemical Society*, *23*, 1579–1584.

Jeong, Y. I., Song, J. G., Kang, S. S., Ryu, H. H., Lee, Y. H., Choi, C., et al. (2003). Preparation of poly(DL-lactide-co-glycolide) microspheres encapsulating all-trans retinoic acid. *International Journal of Pharmaceutics*, *259*, 79–91.

Kim, C., Lee, S. C., & Kang, S. W. (2000). Synthesis and the micellar characteristics of poly(ethylene oxide)-deoxycholic acid conjugates. *Langmuir*, *16*, 4792–4797.

Kim, D. G., Jeong, Y. I., Choi, C., Roh, S. H., Kang, S. K., Jang, M. K., et al. (2006). Retinol-encapsulated low molecular water-soluble chitosan nanoparticles. *International Journal of Pharmaceutics*, *319*, 130–138.

Kim, J. H., Kim, Y. S., Park, K., Kang, E., Lee, S., Nam, H. Y., et al. (2008). Self-assembled glycol chitosan nanoparticles for the sustained and prolonged delivery of antiangiogenic small peptide drugs in cancer therapy. *Biomaterials*, *29*, 1920–1930.

Kim, K., Kwon, S., Park, J. H., Chung, H., Jeong, S. Y., & Kwon, I. C. (2005). Physicochemical characterizations of self-assembled nanoparticles of glycol chitosan-deoxycholic acid conjugates. *Biomacromolecules*, *6*, 1154–1158.

Kumar, M. N. V. R., Muzzarelli, R. A. A., Muzzarelli, C., Sashiwa, H., & Domb, A. J. (2004). Chitosan chemistry and pharmaceutical perspectives. *Chemical Reviews*, *104*, 6017–6084.

Kurita, K., Ikeda, H., Yoshida, Y., Shimojoh, M., & Harata, M. (2002). Chemoselective protection of the amino groups of chitosan by controlled phthaloylation: Facile preparation of a precursor useful for chemical modifications. *Biomacromolecules*, *3*(1), 1–4.

Kurita, K., Shimada, K., Nishiyama, Y., Shimojoh, M., & Nishimura, S.-I. (1998). Nonnatural branched polysaccharides: Synthesis and properties of chitin and chitosan having R-mannoside branches. *Macromolecules*, *31*, 4764–4769.

Kwon, S., Park, J. H., Chung, H., Kwon, I. C., & Jeong, S. Y. (2003). Physicochemical characteristics of self-assembled nanoparticles based on glycol chitosan bearing 5β-cholanic acid. *Langmuir*, *19*, 10188–10193.

Lee, K. Y., Kim, J. H., Kwon, I. C., & Jeong, S. Y. (2000). Self-aggregates of deoxycholic acid modified chitosan as a novel carrier of adriamycin. *Colloid and Polymer Science*, *278*, 1216–1219.

Lee, K. Y., Kwon, I. C., Kim, Y. H., Jo, W. H., & Jeong, S. Y. (1998). Preparation of chitosan self-aggregates as a gene delivery system. *Journal of Controlled Release*, *51*(2–3), 213–220.

Leonard, M., De Boisseson, M. R., Hubert, P., Dalencon, F., & Dellacherie, E. (2004). Hydrophobically modified alginate hydrogels as protein carriers with specific controlled release properties. *Journal of Controlled Release*, *98*(3), 395–405.

Li, Y. Y., Chen, X. G., Yu, L. M., Wang, S. X., Sun, G. Z., & Zhou, H. Y. (2006). Aggregation of hydrophobically modified chitosan in solution and at the air–water interface. *Journal of Applied Polymer Science*, *102*, 1968–1973.

Lira, A., Nanclares, D., Neto, A., & Marchetti, J. (2007). Drug–polymer interaction in the all-trans retinoic acid release from chitosan microparticles. *Journal of Thermal Analysis and Calorimetry*, *87*(3), 899–903.

Liu, C. G., Desai, K. G., Chen, X. G., & Park, H. J. (2005). Linolenic acid-modified chitosan for formation of self-assembled nanoparticles. *Journal of Agricultural Food Chemistry*, *53*(2), 437–441.

Liu, L., Li, Y., Fang, Y. E., & Chen, L. X. (2005). Microwave-assisted graft copolymerization of 3-caprolactone onto chitosan via the phthaloyl protection method. *Carbohydrate Polymers*, *60*, 351–356.

Liu, X. M., Pramoda, K. P., Yang, Y. Y., Chow, S. Y., & He, C. (2004). Cholesteryl-grafted functional amphiphilic poly(N-isopropylacrylamide-co-N-hydroxylmethylacrylamide): Synthesis, temperature-sensitivity, self-assembly and encapsulation of a hydrophobic agent. *Biomaterials*, *25*(13), 2619–2628.

Makuška, R., & Gorochovceva, N. (2006). Regioselective grafting of poly(ethylene glycol) onto chitosan through C-6 position of glucosamine units. *Carbohydrate Polymers*, *64*, 319–327.

Na, K., Park, K. H., Kim, S. W., & Bae, Y. H. (2000). Self-assembled hydrogel nanoparticles from curdlan derivatives: Characterization, anti-cancer drug release and interaction with a hepatoma cell line (HepG2). *Journal of Controlled Release*, *69*(2), 225–236.

Opanasopit, P., Ngawhirunpat, T., Rojanarata, T., Choochottiros, C., & Chirachanchai, S. (2007). N-phthaloylchitosan-g-mPEG design for all-trans retinoic acid-loaded polymeric micelles. *European Journal of Pharmaceutical Sciences*, *30*(5), 424–431.

Osman, Z., & Arof, A. K. (2003). FTIR studies of chitosan acetate based polymer electrolytes. *Electrochimica Acta*, *48*(8), 993–999.

Park, K., Kim, K., Kwon, I. C., Kim, S. K., Lee, S., Lee, D. Y., et al. (2004). Preparation and characterization of self-assembled nanoparticles of heparin-deoxycholic acid conjugates. *Langmuir*, *20*(26), 11726–11731.

Rahman, A., & Brown, C. W. (1983). Effect of pH on the critical micelle concentration of sodium dodecyl sulphate. *Journal of Applied Polymer Science*, *28*, 1331–1334.

Rout, D. K., Pulapura, S. K., & Gross, R. A. (1993). Liquid crystalline characteristics of site-selectively-modified chitosan. *Macromolecules*, *26*, 5999–6006.

Sarmento, B., Ferreira, D., Veiga, F., & Ribeiro, A. (2006). Characterization of insulin-loaded alginate nanoparticles produced by ionotropic pre-gelation through DSC and FTIR studies. *Carbohydrate Polymers*, *66*(1), 1–7.

Sugimoto, M., Morimoto, M., Sashiwa, H., Saimoto, H., & Shigemasa, Y. (1998). Preparation and characterization of water-soluble chitin and chitosan derivatives. *Carbohydrate Polymers*, *36*, 49–59.

Sui, W. P., Song, G. L., Chen, G. H., & Xu, G. Y. (2005). Aggregate formation and surface activity property of an amphiphilic derivative of chitosan. *Colloids and Surface A: Physicochemical and Engineering Aspects*, *256*, 29–33.

Tang, N., Du, G., Wang, N., Liu, C., Hang, H., & Liang, W. (2007). Improving penetration in tumors with nanoassemblies of phospholipids and doxorubicin. *Journal of the National Cancer Institute*, *99*(13), 1004–1015.

Wang, Y. S., Liu, L. R., Jiang, Q., & Zhang, Q. Q. (2007). Self-aggregated nanoparticles of cholesterol-modified chitosan conjugate as a novel carrier of epirubicin. *European Polymer Journal*, *43*, 43–51.

Wang, Y. S., Liu, L. R., Weng, J., & Zhang, Q. (2007). Preparation and characterization of self-aggregated nanoparticles of cholesterol-modified O-carboxymethyl chitosan conjugates. *Carbohydrate Polymers*, *69*, 597–606.

Yang, X. D., Zhang, Q. Q., Wang, Y. S., Chen, H., Zhang, H. Z., Gao, F. P., et al. (2008). Self-aggregated nanoparticles from methoxy poly(ethylene glycol)-modified chitosan: Synthesis; characterization; aggregation and methotrexate release in vitro. *Colloids and Surface B: Biointerfaces*, *61*, 125–131.

Yoksan, R., Akashi, M., Biramontri, S., & Chirachanchai, S. (2001). Hydrophobic chain conjugation at hydroxyl group onto γ-ray irradiated chitosan. *Biomacromolecules*, *2*, 1038–1044.

Yuan, X. B., Li, H., & Yuan, Y. B. (2006). Preparation of cholesterol-modified chitosan self-aggregated nanoparticles for delivery of drugs to ocular surface. *Carbohydrate Polymers*, *65*, 337–345.

Zhang, C., Ping, Q. N., Zhang, H. J., & Shen, J. (2003). Preparation of N-alkyl-O-sulfate chitosan derivatives and micellar solubilization of taxol. *Carbohydrate Polymers*, *54*, 137–141.

Zhang, H. Z., Gao, F. P., Liu, L. R., Li, X. M., Zhou, Z. M., Yang, X. D., et al. (2009). Pullulan acetate nanoparticles prepared by solvent diffusion method for epirubicin chemotherapy. *Colloids and Surface B: Biointerfaces*, *71*, 19–26.